

# Covariation of a Specificity-Determining Structural Motif in an Aminoacyl-tRNA Synthetase and a tRNA Identity Element<sup>†</sup>

Susan A. Hawko and Christopher S. Francklyn\*

Department of Biochemistry, University of Vermont, Health Sciences Complex, Burlington, Vermont 05405

Received November 3, 2000; Revised Manuscript Received December 28, 2000

**ABSTRACT:** Transfer RNA (tRNA) identity determinants help preserve the specificity of aminoacylation in vivo, and prevent cross-species interactions. Here, we investigate covariation between the discriminator base (N73) element in histidine tRNAs and residues in the histidyl-tRNA synthetase (HisRS) motif 2 loop. A model of the *Escherichia coli* HisRS–tRNA<sup>His</sup> complex predicts an interaction between the prokaryotic conserved glutamine 118 of the motif 2 loop and cytosine 73. The substitution of Gln 118 in motif 2 with glutamate decreased discrimination between cytosine and uracil some 50-fold, but left overall rates of adenylation and aminoacylation unaffected. By contrast, substitutions at neighboring Glu 115 and Arg 121 affected both adenylation and aminoacylation, consistent with their predicted involvement in both half-reactions. Additional evidence for the involvement of the motif 2 loop was provided by functional analysis of a hybrid *Saccharomyces cerevisiae*–*E. coli* HisRS possessing the 11 amino acid motif 2 loop of the yeast enzyme. Despite an overall decreased activity of nearly 1000-fold relative to the *E. coli* enzyme, the chimera nevertheless exhibited a modest preference for the yeast tRNA<sup>His</sup> over the *E. coli* tRNA, and preferred wild-type yeast tRNA<sup>His</sup> to a variant with C at the discriminator position. These experiments suggest that part of, but not all of, the specificity is provided by the motif 2 loop. The close interaction between enzyme loop and RNA sequence elements suggested by these experiments reflects a covariation between enzyme and tRNA that may have acted to preserve aminoacylation fidelity over evolutionary time.

Aminoacyl-tRNA synthetases (aaRS)<sup>1</sup> catalyze the ligation of amino acids to their cognate tRNAs, a two-step reaction that contributes to the specificity of translation (1). Each synthetase is confronted by 75 potential tRNA isoacceptor substrates, a selection process described as the tRNA identity problem. Despite extensive work over the past decade which has resulted in the identification of tRNA identity determinants (2), how enzyme elements contribute to tRNA specificity still remains unknown. Crystallographic studies have served to define subclass- and system-specific tRNA recognition features, but the precise mechanistic steps where recognition determinants mediate their effect are still being defined (2, 3).

In this paper, we address the functional significance of a strict evolutionary covariance between the discriminator base (N73) in histidine tRNAs (tRNA<sup>His</sup>) and a discrete peptide

structural element in the motif 2 loop of histidyl-tRNA synthetases (HisRS). HisRS possesses the characteristic antiparallel  $\beta$ -sheet fold (4) and the three diagnostic sequence motifs (denoted motifs 1, 2, and 3) that distinguish class II enzymes (5, 6). Motif 1 comprises part of the dimeric interface, while motifs 2 and 3 contribute conserved charged and polar side chains that dictate the bent conformation of ATP unique to this class of aaRS (7). Of particular importance is a loop element in motif 2 (hereafter the m2 loop) that provides a framework for class-conserved glutamates and arginines.

Motif 2 residues provide electrostatic contacts to the PP<sub>i</sub> leaving group during the first reaction, and critical sequence-specific tRNA interactions in the subsequent transfer step (7). In the aspartyl system, detailed crystal structures (8, 9) and alanine scanning mutagenesis experiments (10) indicate that side chains within motif 2 (Asp 328, Ser329, and Thr331) are responsible for direct contact of G73, with specificity mainly realized at the level of  $k_{\text{cat}}$  (11). The mutagenesis experiments further revealed strong negative thermodynamic coupling ( $\Delta\Delta G_{\text{cat}} = 2.02$  kcal/mol) between these side chains, which may indicate the interdependent nature of the interactions required to correctly position A76. These data and related observations from the seryl- system (12) suggest that ejection of pyrophosphate may be coupled to tRNA binding by the action of the motif 2 loop.

For the histidine system in particular, the transfer step may be highly dependent on interactions made by the enzyme with the –1:73 base pair. Analysis of the identity determi-

<sup>†</sup> This work was supported by NIH Grant GM54899. S.A.H. was supported by an NCI Cancer Biology training fellowship (CA09286).

\* Correspondence should be addressed to this author at the Department of Biochemistry, University of Vermont College of Medicine, Health Sciences Complex, Burlington, VT 05405. E-mail: franck@cmba.uvm.edu, phone: (802) 656-8450, fax: (802) 862-8229.

<sup>1</sup> Abbreviations: aminoacyl-tRNA synthetases are abbreviated as aaRS, with individual enzymes identified by the three-letter code referring to the appropriate amino acid followed by RS; IPTG, isopropyl 1-thio- $\beta$ -D-galactopyranoside; Ni-NTA, nickel nitrilotriacetic acid; PCR, polymerase chain reaction;  $\beta$ -ME, 2-mercaptoethanol; *E. coli*, *Escherichia coli*; *S. cerevisiae*, *Saccharomyces cerevisiae*; DTT, dithiothreitol; NTP, nucleotide triphosphate; ATP, adenosine triphosphate; GMP, guanosine monophosphate; NaPP<sub>i</sub>, sodium pyrophosphate; PP<sub>i</sub>, inorganic pyrophosphate.

nants of tRNA<sup>His</sup> in both *E. coli* and *S. cerevisiae* systems suggests that the  $-1:73$  base pair and the anticodon trinucleotides serve as the principal recognition elements, with the following differences. Loss of G-1 is associated with a 230-fold decreased  $k_{\text{cat}}$  in *E. coli*, and a relative 500-fold decrease in yeast (13, 14). Discriminator base substitutions bring about approximately 10–100-fold decreases in bacteria and somewhat less of an effect in yeast tRNA (13, 15). In general, substitutions at  $-1:73$  are preferentially associated with decreases in  $k_{\text{cat}}$  rather than increases in  $K_{\text{m}}$ . By contrast, the anticodon is a weaker but nonetheless significant identity determinant, and substitutions of G34 and U35 typically impose 5-fold decreases in binding, as measured both by  $K_{\text{m}}$  and by  $K_{\text{d}}$  (14–16). The histidine tRNA synthetase is also notable for its ability to aminoacylate RNA structures possessing acceptor stem determinants alone in a variety of contexts, including mini- and microhelices (17, 18) and tRNA-like domains from plant viruses (19). Owing to the close proximity of  $-1:73$  to A76, this raises the question of how recognition of 73 is integrated with the amino acid transfer step.

In the work described below, this question is approached by consideration of the apparent covariation of the identity of the discriminator base with sequences located in the motif 2 loop of HisRS. The discriminator base shows a distinct pattern of conservation, with prokaryotic histidine tRNAs containing C73, and archaeal and eukaryotic tRNAs containing A73 (20). This pattern of conservation is mirrored in the enzymes, with the prokaryotic homologues sharing a conserved glutamine at position 118, and the eukaryotic enzymes replacing this residue with an Ala-Met-Thr tripeptide motif (21). Here, the functional significance of this apparent covariation is addressed by probing the requirement for Gln 118 in discriminator base specificity and by analysis of the properties of a chimeric prokaryotic HisRS containing a eukaryotic motif 2 loop.

## MATERIALS AND METHODS

**Construction of Mutant Proteins.** Mutant HisRS proteins were constructed using published modifications of the Kunkel procedure (14, 21). Mutagenic oligonucleotides (Operon) were designed with randomized codons at positions corresponding to amino acids 115 and 118, and by direct changes for 121 and the m2 loop swap mutants. The HisRS mutants were cloned via an intermediate step using the TA-vector (Invitrogen) in the pQE-30 expression vector (Qiagen) as previously described (21). Construction of the M162A mutant was then carried out using the Quick-Change mutagenesis procedure (Stratagene). All mutations introduced were verified by sequencing using an ABI-381 sequencer.

**Protein Expression and Purification.** Purification of wt HisRS was carried out as described previously (22). Overexpression and purification of all mutant hexahistidine-tagged HisRS proteins were carried out as previously described (21). Final Ni-NTA agarose peak fractions were concentrated (Amicon filter cell and Centricon concentrators) and retained at  $-20^{\circ}\text{C}$  in storage buffer (100 mM Tris•HCl, pH 7.0, 100 mM NaCl, 1 mM  $\beta$ -ME, and 40% glycerol). Concentrations of all HisRS stocks were determined by absorbance at 280 nm, using an extinction coefficient of  $127\,097\text{ M}^{-1}\text{ cm}^{-1}$ .

**tRNA Transcription and Purification.** In vitro transcripts of C73 and U73 *E. coli* tRNA<sup>His</sup> sequences were prepared

as described previously (14, 16). The A73 *E. coli* transcripts were constructed as an annealed tRNA (23, 24). A 19-mer oligonucleotide corresponding to the 3' end of tRNA<sup>His</sup> was synthesized by Dharmacon Research (Boulder, CO) encoding the corresponding A73 nucleotide. T<sub>7</sub> RNAP transcription of a Taq<sup>q</sup>I linearized plasmid containing the wt *E. coli* tRNA<sup>His</sup> sequence generated the 3/4 length molecule to which the 3' oligo was annealed to create the full-length A73 tRNA<sup>His</sup>. *S. cerevisiae* tRNA<sup>His</sup> transcripts were prepared from a plasmid generously provided by Richard Geigé, CNRS, Strasbourg. The yeast (C73) tRNA<sup>His</sup> transcript was prepared following Quick Change mutagenesis (Stratagene) of N73. Following purification of in vitro T<sub>7</sub> transcripts on 7 M urea/12.5% acrylamide gels, tRNAs were collected by electroelution (Bio-Rad Elu-Trap) prior to ethanol precipitation. Transcripts were quantitated by absorbance at 260 nm ( $1\text{ AU} = 33\text{ }\mu\text{g mL}^{-1}$ ) and by subsequent activity assay to determine the concentration of functional molecules. Total yeast tRNA (baker's yeast) was supplied by Boehringer-Roche. The final concentration of total yeast tRNA was approximated in units of milligrams per milliliter to correspond to the molar concentrations used for the other yeast transcripts. Purified *E. coli* tRNA<sup>Thr</sup> was the generous gift of Anne Catherine Dock Bergeon, IGBMC, Strasbourg. Yeast tRNA<sup>Asp</sup> template plasmid was supplied by R. Giegé.

**Enzyme Assays.** Pyrophosphate exchange reactions were performed as previously described (21) using enzyme concentrations of 10 nM. Aminoacylation of tRNA<sup>His</sup> transcripts was carried out under standard conditions described previously (10, 14, 21). Wild-type untagged HisRS has been shown previously to have the same kinetic parameters as the hexahistidine-tagged enzyme (14, 25). Enzyme concentrations of 10 nM were used for aminoacylation of C73 transcripts by wild-type and single loop substitution mutant proteins, while higher concentrations (500 nM) were required by the yeast loop substituted enzymes (ScM2L.HRS and M162A-SL.HRS). Aminoacylation of U73 and yeast transcripts required enzyme concentrations of wild-type and single loop substitution mutants at 100 nM, while ScM2L.HRS required 500 nM concentrations. Concentration ranges of 0.5–5  $\mu\text{M}$  in *E. coli* transcript were used for assays with single substitution HisRS mutants, and 0.5–50  $\mu\text{M}$  for ScM2L.HRS charging of both *E. coli* and yeast tRNA<sup>His</sup>. Kinetic constants were determined by fitting of the data to the Michaelis–Menten equation as implemented by the Kaleidagraph package (Synergy Software version 3.08d). Comparative aminoacylation of yeast tRNAs was carried out using a fixed concentration of tRNA, 200  $\mu\text{g/mL}$  bulk yeast tRNA, and 2.5  $\mu\text{M}$  yeast C73 tRNA<sup>His</sup>, and an enzyme concentration of 200 nM for both wt HisRS and ScM2L.HRS. All kinetic parameters reported represent the mean of at least two, and often three, independent determinations.

## RESULTS

**Predicting Discriminator Base Contacts from a Model of the HisRS–tRNA<sup>His</sup> Complex.** As a first approach to understanding the molecular basis of discriminator base recognition, a docking model between HisRS and tRNA<sup>His</sup> was created by superposition of HisRS and the yeast AspRS–tRNA<sup>Asp</sup> complex, with the subsequent deletion of atoms corresponding to AspRS (Figure 1). The general features of this model have been described previously (4, 14) and agree

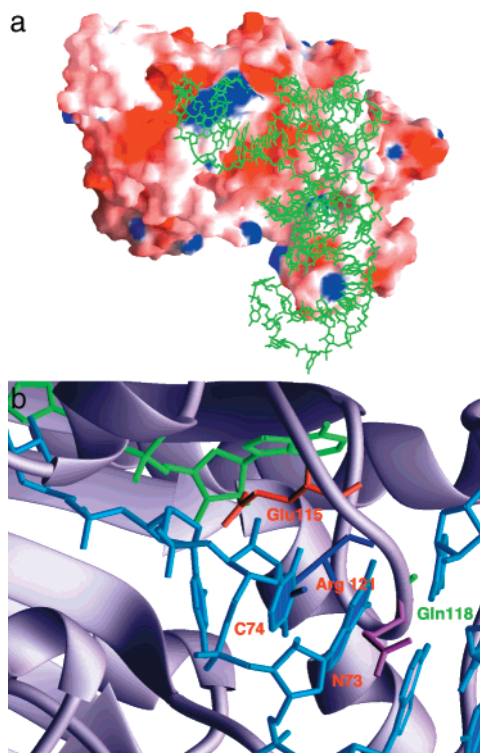


FIGURE 1: Molecular modeling of HisRS-tRNA<sup>His</sup> interactions. (a) GRASP (40) model of dimeric HisRS complex with yeast tRNA<sup>Asp</sup>, which serves as a proxy for the authentic tRNA<sup>His</sup>. The model was constructed by superimposing the coordinates for the  $\alpha$  carbons of the catalytic domains of *E. coli* HisRS and the yeast AspRS-tRNA<sup>Asp</sup> complex, and then using the resulting position of tRNA<sup>Asp</sup> to approximate the approach of tRNA<sup>His</sup> to the active site. Only one tRNA molecule is shown for clarity. The tRNA lies across the dimeric interface, but makes most of its contacts to one monomer by interacting with an extended region of positive potential that runs diagonally from the active site to the C-terminal domain. (b) Close-up of the active site showing predicted interactions between the motif 2 loop and acceptor stem. The histidyl-adenylate is rendered in green and the tRNA in cyan. No attempt has been made to model the position or interactions of G-1, which is not included in this model.

with recent footprinting data (16). As this model is not based on crystallographic data, the positions of nucleotides and side chains are only approximations and do not reflect the possibility that specific conformational changes in HisRS active site polypeptide segments (such as the m2 loop) may be associated with tRNA binding. With this caveat in mind, examination of the model allows the formulation of specific predictions concerning the discriminator base and the m2 loop that are amenable to experimental test. First, we find that Q118 is in close proximity to the G-1:C73 base pair, creating the potential for a bidendate interaction in which

the O $\epsilon$ 1 of the side chain accepts a hydrogen bond from N4 of C73, while N $\epsilon$ 1 donates a hydrogen bond to O6 of G-1. Such an interaction would be predicted to be specific for prokaryotic HisRS. The HisRS motif 2 loop is also predicted to make the class II conserved tRNA contacts, which in this case include direct hydrogen bonds made by Arg 121 to C74, and the interaction between Glu 115 and the ribose of C74. In the model, Glu 115 is shown pointing into the active site to interact with N7 of ATP, but a side chain rotation around  $\chi$ 1 and  $\chi$ 2 would allow for interactions between  $\epsilon$  oxygens and the 2' hydroxyl group. These potential interactions were probed by oligonucleotide mutagenesis, substituting Q118 with glutamate, R121 with histidine, and E115 with alanine or aspartate. These conservative substitutions alter side chain chemistry and hydrogen bonding potential with minimal impact on structure. The resulting mutant proteins were expressed and purified to the high yields characteristic of the wild-type enzyme.

**Single Residue Motif 2 Loop Substitutions Alter Discriminator Base Recognition.** On the basis of the HisRS-tRNA<sup>His</sup> docking model, a conservative substitution of Q118 would be predicted to reduce discrimination at N73 with minimal impact on adenylate synthesis. The converse prediction would hold true for substitutions at R121 and E115, which are predicted to contact C74. These hypotheses were tested using the pyrophosphate exchange assay, which measures the rate of histidine activation. Table 1 shows that the primary effect of the E115D,A and R121H substitutions was to reduce the turnover rate of pyrophosphate exchange ( $k_{\text{cat}}$ ) by 2-, 33-, and 33-fold, respectively, while the Q118E substitution had no effect ( $<2$ -fold) on PP<sub>i</sub> exchange. All mutants showed only slight ( $\leq 2$ -fold) effects on  $K_m$ . These results are consistent with the predictions described above and the behavior of E115 and R121 in previously reported HisRS complexes (4, 26).

The m2 loop single mutants were subsequently analyzed in aminoacylation assays using the wild-type *E. coli* C73 tRNA<sup>His</sup> and mutant *E. coli* U73 tRNA<sup>His</sup> transcripts. Altered aminoacylation specificity for the discriminator base would be indicated in these assays as alterations in the ratio of activity ( $k_{\text{cat}}/K_m$ ) on wild-type and mutant transcripts. As shown in Table 2, the  $k_{\text{cat}}$  for aminoacylation of the wild-type transcript was diminished 5- and 6.6-fold with E115D,A and Q118E, and nearly 17-fold with R121H. Michaelis constants were virtually unaltered, except for a 5-fold increase with R121H. The greater effects on  $k_{\text{cat}}$  relative to  $K_m$  are consistent with previous data showing tRNA binding is insensitive to discriminator base changes (16). Differences in discriminator base sensitivity were subsequently revealed

Table 1: Steady-State PP<sub>i</sub> Exchange Kinetics of Single Site Substitution HisRS Mutants<sup>a</sup>

	$K_m$ ( $\mu\text{M}$ )		$k_{\text{cat}}$ ( $\text{s}^{-1}$ )		$k_{\text{cat}}/K_m$ ( $\times 10^6 \text{ M}^{-1} \text{ s}^{-1}$ )	
	1 His	2 ATP	3 His	4 ATP	5 His	6 ATP
wt.HRS	35.4 $\pm$ 3.7	675 $\pm$ 78	133 $\pm$ 2.2	203 $\pm$ 5.2	3.76	0.30
E115A	26.8 $\pm$ 8.9	276 $\pm$ 77	5.8 $\pm$ 0.3	7.2 $\pm$ 0.4	0.22	0.03
E115D	50.4 $\pm$ 8.7	971 $\pm$ 112	30.7 $\pm$ 1.0	101.8 $\pm$ 2.6	0.61	0.10
Q118E	17.0 $\pm$ 3.1	575 $\pm$ 128	170 $\pm$ 4.5	160.2 $\pm$ 3.4	10.0	0.28
R121H	46.3 $\pm$ 19	703 $\pm$ 226	3.65 $\pm$ 0.27	7.3 $\pm$ 0.3	0.08	0.01

<sup>a</sup> Assays were performed at 37 °C, as described under Materials and Methods. Values shown represent the mean and standard deviations of three independent assays.



Table 2: Steady-State Aminoacylation Kinetics of Single Amino Acid Substitution HisRS Mutants<sup>a</sup>

	$K_m$ ( $\mu$ M)		$k_{cat}$ ( $s^{-1}$ )		$k_{cat}/K_m$ ( $\times 10^6$ $M^{-1} s^{-1}$ )	
	7 wild type <sup>b</sup>	8 U73	9 wt	10 U73	11 wt	12 U73
wt.HRS <sup>c</sup>	0.34 $\pm$ 0.05	0.19 $\pm$ 0.04	1.71 $\pm$ 0.06	0.03 $\pm$ 0.001	5.03	0.16
E115A	0.94 $\pm$ 0.52	0.15 $\pm$ 0.03	0.30 $\pm$ 0.06	0.04 $\pm$ 0.001	0.32	0.27
E115D	0.65 $\pm$ 0.23	0.32 $\pm$ 0.09	0.63 $\pm$ 0.07	0.07 $\pm$ 0.004	0.97	0.22
Q118E	0.37 $\pm$ 0.09	1.13 $\pm$ 0.55	0.26 $\pm$ 0.02	0.13 $\pm$ 0.02	0.70	0.12
R121H	1.53 $\pm$ 0.38	0.62 $\pm$ 0.07	0.10 $\pm$ 0.01	$2 \times 10^{-4}$	0.07	$3 \times 10^{-4}$

<sup>a</sup> Assays were performed at 37 °C, as described under Materials and Methods. <sup>b</sup> C73 tRNA<sup>His</sup> is the wild-type (wt) substrate for HisRS. <sup>c</sup> wt.HRS represents the wild-type version of the enzyme.

using the U73 transcript of *E. coli* tRNA<sup>His</sup>. As determined from comparisons of the catalytic specificity (the ratio of  $k_{cat}/K_m$  on the C73 transcript versus U73 transcript), these assays showed that substitutions of both Glu 115 and Gln 118 were associated with decreased specificity at N73. The most marked decline was observed for E115A (with ratios from 31 for wt to 1.2 for the mutant), while E115D and Q118E exhibited ratios of 4.4 and 5.8, respectively (Table 2). When compared on the basis of  $k_{cat}$ , the drop in the ratio of activities on the two transcripts was most pronounced for the Q118E mutant, from 68-fold to less than 2-fold. By contrast, R121H showed a 233-fold increase relative to the wild-type ratio of transcript activities. These observed changes are consistent with the role of Q118 as a direct contact residue for C73, but also raise the possibility of a role for Glu 115 in determining discriminator base specificity. The increased specificity exhibited by R121H illustrates that the loss of the contact to N73 by virtue of the base change and the loss of the contact to C74 by the side chain substitution are thermodynamically coupled, with a  $\Delta\Delta G_{k_{cat}}$  of 2.02 kcal/mol. Thus, these two interactions are not independent of each other.

**A *S. cerevisiae* m2 Loop–*E. coli* HisRS Chimera That Decreases the Cross-Species Aminoacylation Barrier.** The experiments described above provided experimental evidence for the proposed interaction between residues in the m2 loop and the discriminator base. Were this to be true, it is reasonable to expect that the corresponding polypeptide segment in the yeast HisRS provides similar discrimination for G-1:A73 in the yeast tRNA<sup>His</sup>. [Although the corresponding yeast tRNA<sup>His</sup> has only 37 of 76 nucleotides in common with *E. coli* tRNA<sup>His</sup> (Figure 2b), transplantation experiments indicate that the G-1:A73 base pair and GUG anticodon are sufficient to confer efficient histidylolation by yeast HisRS (27).] As a direct test of this proposition, we constructed a chimeric version of *E. coli* HisRS (ScM2L.HRS), in which 9 residues of the prokaryotic m2 loop were substituted with the corresponding 11 residues of *Saccharomyces cerevisiae* (Figure 2a,c). Of the 11 substituted residues, 7 introduced changes in the *E. coli* m2 loop sequence to mimic the yeast enzyme. In particular, the glutamine at position 118 was substituted by the sequence Ala-Met-Thr (Figure 2c).

The adenylation and aminoacylation functions of the ScM2L.HRS mutant protein were analyzed as described above, utilizing *E. coli* and yeast tRNA transcripts as well as total yeast tRNA to make specificity comparisons. ScM2L.HRS exhibited a 65.8-fold decrease in the turnover rate for pyrophosphate exchange (data not shown), implying that the overall retention of catalytic function was accompanied by the loss of one or more favorable contacts to

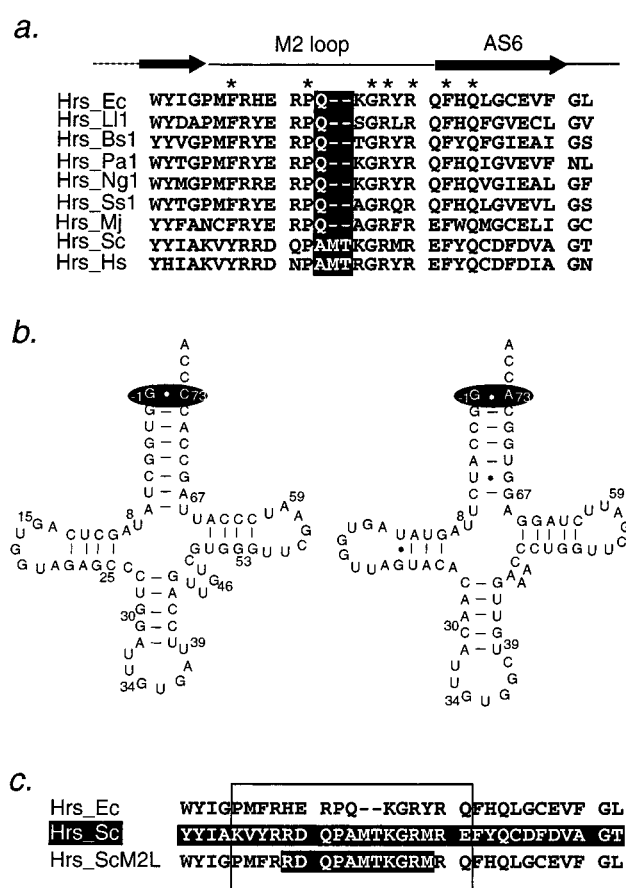


FIGURE 2: Design of loop swap mutants. (a) Sequence alignment of eight HisRS (Hrs) protein sequences. Organisms are abbreviated as follows: Ec (*E. coli*), Sc (*S. cerevisiae*), Hs (*Homo sapiens*), Ll1 (*Lactococcus lactis*), Bs (*Bacillus subtilis*), Pa (*Pseudomonas aurelias*), Ng (*Neisseria gonorrhoeae*), Ss (*Synechocystis* PCC6803), Mj (*Methanococcus jannaschii*). Secondary structure is indicated above the sequences; asterisks indicate conserved positions. Position 118 is highlighted in reverse type. (b) Sequences of representative prokaryotic (*E. coli*) and eukaryotic (*S. cerevisiae*) tRNA<sup>His</sup> corresponding to the unmodified transcripts. N73 is highlighted by the ovals located in the respective acceptor stems. (c) Derivation of the loop swap mutant (ScM2L.HRS) from *E. coli* and yeast motif 2 loop sequences. Yeast HisRS sequence is shown in reverse type. The boxed region highlights the m2 loop.

ATP. ScM2L.HRS also displayed markedly reduced aminoacylation activity on the wild-type transcript, with a 27.6-fold increase in  $K_m$  and a 700-fold decrease in  $k_{cat}$  relative to wild type (Table 3). However, subsequent experiments comparing the activities of the native *E. coli* enzyme to the chimera on a set of *E. coli* and yeast histidine tRNA transcripts provided evidence of altered specificity. Analysis of the aminoacylation of full-length transcripts of *E. coli* C73

Table 3: Aminoacylation Parameters of *E. coli* and Yeast Transcripts<sup>a</sup> by ScM2L.HRS and *E. coli* wt.HisRS

	<i>E. coli</i> wt <sup>b</sup> tRNA <sup>His</sup>			<i>E. coli</i> A73 tRNA <sup>His</sup>			yeast wt <sup>b</sup> tRNA <sup>His</sup>		
	$K_m$ ( $\mu$ M)	$k_{cat}$ (s <sup>-1</sup> )	$k_{cat}/K_m$ (M <sup>-1</sup> s <sup>-1</sup> )	$K_m$ ( $\mu$ M)	$k_{cat}$ (s <sup>-1</sup> )	$k_{cat}/K_m$ (M <sup>-1</sup> s <sup>-1</sup> )	$K_m$ ( $\mu$ M)	$k_{cat}$ (s <sup>-1</sup> )	$k_{cat}/K_m$ (M <sup>-1</sup> s <sup>-1</sup> )
<i>E. coli</i> wt.HRS	9.4 ± 0.2	1.4 ± 0.1	4.24 × 10 <sup>6</sup>	6.6 ± 0.16	0.1 ± 0.02	1.49 × 10 <sup>4</sup>	0.72 ± 0.1	2.3 × 10 <sup>-4</sup>	319
ScM2L.HRS	9.1 ± 2.1	2.8 × 10 <sup>-3</sup>	308	2.03 ± 0.06	2.6 × 10 <sup>-4</sup>	127	1.39 ± 0.4	5.4 × 10 <sup>-4</sup>	388
M162A-SL.HRS	3.7 ± 0.2	8.5 × 10 <sup>-4</sup>	230	7.5 ± 0.8	2.6 × 10 <sup>-4</sup>	35	nd	nd	nd

<sup>a</sup> The *E. coli* transcripts used were annealed tRNAs, while the yeast transcripts were full-length. All assays were carried out at 37 °C. <sup>b</sup> In *E. coli* wt tRNA<sup>His</sup>, the wt discriminator base is C, while in the wild-type yeast tRNA<sup>His</sup>, the discriminator base is A. Standard deviations are given where calculated; for other parameters, the error was within 10% of the indicated values. nd = not detected; aminoacylation of yA73 transcripts was undetectable for this mutant.

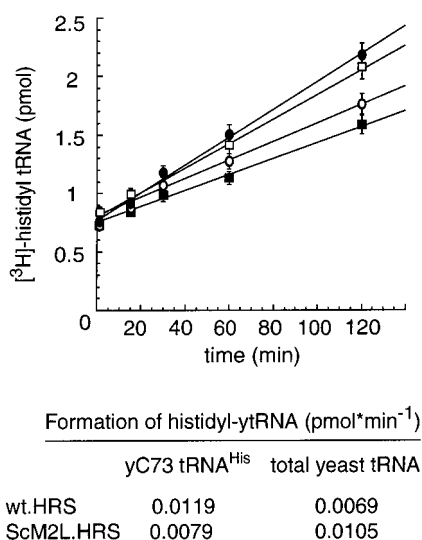


FIGURE 3: Comparative aminoacylation of yeast tRNAs. Initial rate assays were performed using 200  $\mu$ g/mL bulk yeast tRNA or 2.5  $\mu$ M C73 yeast tRNA<sup>His</sup> transcript, and 200 nM enzyme concentrations, as described under Materials and Methods: (●) *E. coli* HisRS, yeast C73 tRNA<sup>His</sup>; (□) ScM2L.HRS, bulk yeast tRNA; (○) ScM2L.HRS, yeast C73 tRNA<sup>His</sup>; (■) *E. coli* HisRS, bulk yeast tRNA. The table gives rates of histidyl-tRNA formation derived from the slopes of the linear fits shown.

and A73 tRNA<sup>His</sup>, as well as yeast wt (A73) tRNA<sup>His</sup>, showed that the chimera possessed a reduced discrimination between C73 and A73 in the context of the *E. coli* tRNA, but nonetheless aminoacylated the yeast transcript with an efficiency comparable to the *E. coli* enzyme (388 vs 319 M<sup>-1</sup> s<sup>-1</sup>). To further probe specificity differences between the chimera and the native *E. coli* enzyme, additional assays were performed using total yeast tRNA and a full-length yeast tRNA<sup>His</sup> transcript with a C73 substitution. The relatively poor aminoacylation of these substrates by both enzymes precluded a full determination of kinetic parameters, but assays performed at fixed tRNA concentrations (200  $\mu$ g/mL for total yeast tRNA and 2.5  $\mu$ M for yeast C73 tRNA<sup>His</sup>) showed that the chimera was 1.5-fold more active on total yeast tRNA than *E. coli* wt HisRS and 1.5-fold less active on yeast C73 tRNA<sup>His</sup> (Figure 3). As shown by the error bars in these measurements, these differences were repeatable and significant. Additional control experiments using yeast tRNA<sup>Asp</sup> and *E. coli* tRNA<sup>Thr</sup> showed no aminoacylation, indicating that ScM2L.HisRS does not aminoacylate non-cognate tRNAs (data not shown). Thus, the *E. coli* wt and yeast chimeric enzymes have opposite preferences for these two yeast substrates, indicating that introduction of the yeast m2 loop altered the specificity of tRNA aminoacylation. As an additional investigation of the influence of the yeast loop,

the methionine of the AMT tripeptide was substituted with alanine. If the loop is making contact with the discriminator, one would predict a change in the relative preference for A vs C. As shown in Table 3, the alanine substitution had a greater effect on aminoacylation of the *E. coli* A73 tRNA versus the wt C73 *E. coli* tRNA. This is consistent with the proposed role of the AMT tripeptide in conferring specificity for A73. Although assays with the mutant were also performed with yeast tRNA, the aminoacylation of these substrates was below the threshold of accurate quantitation.

The introduction of the yeast m2 loop into the *E. coli* enzyme context is therefore accompanied by a substantial reduction of the thermodynamic barrier between aminoacylation of *E. coli* and yeast histidine tRNAs, and a modest but detectable change in preference for yeast tRNA with A73 vs C73. However, the relatively inefficient rescue of yeast tRNA charging observed in the chimera indicates that sequences outside of the m2 loop must also be critical for aminoacylation of the yeast tRNA.

## DISCUSSION

The high fidelity of the modern day translational apparatus is in part a reflection of the long period of co-evolution between the transfer RNAs and cognate aaRS. While identity determinants in some tRNA families are highly conserved in all three kingdoms, there are numerous examples of kingdom-specific differences (2), as in the conservation of G-1:C73 in prokaryotic histidine tRNAs and G-1:A73 in eukaryotic and archaeal histidine tRNAs (20). By contrast, the precise tRNA synthetase amino acid determinants responsible for recognizing these identity elements are less well characterized, and their conservation has not been addressed. Two different lines of evidence that the HisRS m2 loop is involved in discrimination at N73 have been presented here. These studies were undertaken to test predictions of a model of the HisRS–tRNA<sup>His</sup> complex in which side chains in the motif 2 loop are positioned close to acceptor stem nucleotides, creating the potential for base-specific interactions with the discriminator base. In all complexes of class II enzymes with their cognate tRNAs (8, 9, 12, 24, 28–31), the m2 loop is in close proximity to the discriminator base. However, direct contacts to the discriminator base are not always observed, as in the case of threonyl-tRNA synthetase (31). Comparison of these crystal structures suggests that the approach of the acceptor stem to the active site in Class II aaRS typically involves recognition of the acceptor stem major groove, with the CCA end assuming an extended conformation (26). Differences between these complexes suggest that direct side chain–

base interactions predicted on the basis of homology modeling should be considered as provisional candidates only. In particular, homology models are limited by their inability to predict specific conformational changes required by both the synthetase and the tRNA. With these caveats in mind, alignments between the HisRS motif2 and those of *E. coli* AspRS and *T. thermophilis* SerRS predict a role for Gln 118 in discriminator base recognition (10, 12).

In agreement with our model and these other systems, our experiments showed that single site substitutions of both Glu 115 and Gln 118 reduced discrimination between C and U at base 73, raising the possibility that either or both of these residues are involved in specificity determination. At the level of the kinetic constant  $k_{\text{cat}}$ , Q118E showed the highest activity on the noncognate U73 substrate, suggesting that this side chain is particularly important in specifying the discriminator (Table 2). Such a role for Gln 118 would be consistent with its alignment with the discriminator base contact in other class II tRNA synthetases (e.g., Gln 118 of HisRS aligns with Arg 222 of *E. coli* AspRS, which is responsible for contacts to G73), and its covariation with the discriminator base, both of which undergo substitution in the eukaryotes. A marked reduction in discriminator preference was also observed for substitutions of Glu 115, particularly E115A (Table 2). In contrast to Gln 118, however, Glu 115 is conserved across all HisRS as a universal ATP contact. The fact that Gln 118 and Glu 115 both affect synthetase preference for N73 could be due to the fact that both residues are responsible for direct contacts or, more likely, they participate in a network of hydrogen bonding interactions that acts to enforce the correct positioning of side chains involved in interactions with RNA. This latter effect could explain the apparent increased specificity of R121H for C73, when a comparative analysis with other class II synthetases suggests that Arg 121 (histidine in some class II enzymes) makes a class II conserved interaction with C74 (12, 32). The approximately 2 kcal of coupling energy calculated from the free energy difference between the sum of the individual mutants and the combination of the R121H HisRS and U73 mutant tRNA strongly suggests that contacts to C73 and C74 are not independent of each other. This lack of independence may be due to the fact that all of these interactions ultimately serve to position A76 for amino acid transfer, and defects in one contact can be at least partially compensated by modifications of others.

Previous studies of the recognition of tRNA<sup>His</sup> in *E. coli* and *S. cerevisiae* highlighted characteristic differences between the two systems (15, 25, 27). In general, recognition of the prokaryotic tRNA appeared to be more sensitive to the precise nature of the discriminator base, with recognition of the anticodon serving to mediate binding specificity. By contrast, transplantation experiments of histidine determinants into a tRNA<sup>Asp</sup> context implied that the presence of G-1 serves as the major determinant in eukaryotes, with the anticodon playing a more important role than in the case of the prokaryotes (27). Differences between prokaryotic and eukaryotic tRNA recognition were addressed in our studies here by functional analysis of a chimera in which the yeast motif 2 loop was introduced into *E. coli* HisRS. The first conclusion from this analysis is that introduction of the yeast loop was accompanied by a more significant drop in aminoacylation than in adenylation function (Table 3). The

observation of decreases in both half-reactions suggests the possibility of steric or electrostatic clashes between the yeast residues and the *E. coli* active site, with these serving to collectively impede loop function during the reaction. This effect is magnified in the aminoacylation reaction, indicating a requirement for additional interactions between the loop and other parts of the active site.

Despite the observed decrease in overall aminoacylation, comparative analysis on different substrates indicated a slight but readily detectable alteration in tRNA preference on the part of the chimera. Most notably, the chimera aminoacylated bulk yeast tRNA and wt yeast tRNA<sup>His</sup> transcript more efficiently than the *E. coli* enzyme, and showed a different preference order with respect to the two yeast tRNA substrates differing at the discriminator base (Figure 3). While modest in magnitude, the trend of these differences is consistent with the yeast motif 2 loop contributing to tRNA specificity in the yeast system, as opposed to merely decreasing activity on all substrates. While there are few data about the role of specific contact residues in the yeast enzyme, prior studies indicate that the preference of the wild-type enzyme for G-1:A73 over G-1:C73 is only severalfold (15). The data presented here with respect to M162A-SL.HRS are consistent with a role for the motif 2 loop AMT tripeptide in eukaryotic HisRS in providing specificity for A73. The failure of the yeast motif 2 loop transplantation to more fully rescue aminoacylation of the yeast tRNA suggests that other domains in the yeast enzyme responsible for tRNA contact may be necessary for full activity. At a minimum, potential candidate sequences are likely to include the 3<sub>10</sub> helix that forms the HisRS version of the "flipping loop", the long loop in eukaryotic HisRS enzymes between strands AS8 and AS9, and the anticodon binding domain (4). This could be tested by the construction of additional yeast-*E. coli* chimeras, but such mutants would naturally be subject to a host of potential stability and folding problems.

Systematic analysis of tRNA identity determinants suggests that the importance of the discriminator base to many tRNA systems is widespread, but examples of covariations between aaRS and N73 are less common. One reason may be that less selective pressure exists for compensatory amino acid substitutions when the discriminator base is a weaker identity determinant. Previous efforts to demonstrate covariance between m2 loop residues and the discriminator base by loop exchange experiments have been described for the lysyl- and the prolyl- systems (33–35). The discriminator base is a relatively minor determinant in the prokaryotic families for these enzymes, and even less significant for their eukaryotic counterparts (30, 34, 35). More success in converting aaRS specificity for other tRNAs has been achieved by targeting other tRNA identity elements, including the G-1:C72 base pair in tyrosine tRNAs (36) and nucleotide 34 in isoleucine and methionine tRNAs (37). In the latter case, the substituted peptide region was implicated in anticodon recognition by other independent experimental approaches. Two essential criteria for success in such peptide swapping experiments may be that the identity determinant involved constitutes a significant barrier to heterologous aminoacylation, and that the corresponding peptide region be involved in direct contact with that identity determinant.

The precise mechanistic step in the histidine system at which discriminator base contact mediates discrimination



remains to be elucidated. Previously, we have shown that recognition of the discriminator base does not occur at initial tRNA binding steps, which appear instead to be dominated by interactions with the anticodon (14, 16). The data presented here and in previous studies suggest that discriminator base recognition is reflected in the rate-determining step(s) monitored by  $k_{\text{cat}}$ , which could include conformational changes preceding the transfer step or product release. Prior single turnover and recent pre-steady-state kinetic studies conducted in other systems support the idea that the transfer step is rate limiting (38, 39). Continuing studies are likely to focus on the question of how recognition of multiple specificity-determining nucleotides is integrated at the transfer step to provide the necessary biological specificity.

## ACKNOWLEDGMENT

We thank Karin Musier-Forsyth (University of Minnesota, Minneapolis, MN) and Mark Rould (University of Vermont, Burlington, VT) for their helpful comments on the manuscript. Additional thanks are extended to Tim Hunter (Vermont Cancer Center DNA Sequencing Facility, University of Vermont, Burlington, VT) for his expertise and assistance.

## REFERENCES

1. Carter, C. W., Jr. (1993) *Annu. Rev. Biochem.* 62, 715–748.
2. Giegé, R., Sissler, M., and Florentz, C. (1998) *Nucleic Acids Res.* 26, 5017–5035.
3. Cusack, S. (1997) *Curr. Opin. Struct. Biol.* 7, 881–889.
4. Arnez, J. G., Harris, D. C., Mitschler, A., Rees, B., Francklyn, C. S., and Moras, D. (1995) *EMBO J.* 14, 4143–4155.
5. Cusack, S., Berthet-Colominas, C., Härtlein, M., Nassar, N., and Leberman, R. (1990) *Nature* 347, 249–255.
6. Eriani, G., Delarue, M., Poch, O., Gangloff, J., and Moras, D. (1990) *Nature* 347, 203–206.
7. Arnez, J. G., and Moras, D. (1997) *Trends Biochem. Sci.* 22, 211–216.
8. Cavarelli, J., Rees, B., Thierry, J. C., and Moras, D. (1993) *Biochimie* 75, 1117–1123.
9. Cavarelli, J., Eriani, G., Rees, B., Ruff, M., Boeglin, M., Mitschler, A., Martin, F., Gangloff, J., Thierry, J. C., and Moras, D. (1994) *EMBO J.* 13, 327–337.
10. Eriani, G., and Gangloff, J. (1999) *J. Mol. Biol.* 291, 761–773.
11. Pütz, J., Puglisi, J. D., Florentz, C., and Giegé, R. (1991) *Science* 252, 1696–1699.
12. Cusack, S., Yaremchuk, A., and Tukalo, M. (1996) *EMBO J.* 15, 2834–2842.
13. Himeno, H., Hasegawa, T., Ueda, T., Watanabe, K., Miura, K., and Shimizu, M. (1989) *Nucleic Acids Res.* 17, 7855–7863.
14. Yan, W., Augustine, J., and Francklyn, C. (1996) *Biochemistry* 35, 6559–6568.
15. Nameki, N., Asahara, H., Shimizu, M., Okada, N., and Himeno, H. (1995) *Nucleic Acids Res.* 23, 389–394.
16. Bovee, M. L., Yan, W., Sproat, B. S., and Francklyn, C. S. (1999) *Biochemistry* 38, 13725–13735.
17. Francklyn, C., Musier-Forsyth, K., and Schimmel, P. (1992) *Eur. J. Biochem.* 206, 315–321.
18. Francklyn, C., and Schimmel, P. (1990) *Chem. Rev.* 90, 1327–1342.
19. Rudinger, J., Hillenbrandt, R., Sprinzl, M., and Giege, R. (1996) *EMBO J.* 15, 650–657.
20. Sprinzl, M., Horn, C., Brown, M., Ioudovitch, A., and Steinberg, S. (1998) *Nucleic Acids Res.* 26, 148–153.
21. Francklyn, C., Adams, J., and Augustine, J. (1998) *J. Mol. Biol.* 280, 847–858.
22. Francklyn, C., Harris, D., and Moras, D. (1994) *J. Mol. Biol.* 241, 275–277.
23. Wolfson, A. D., Pleiss, J. A., and Uhlenbeck, O. C. (1998) *RNA* 4, 1019–1023.
24. Liu, H., Yap, L. P., Stehlin, C., and Musier-Forsyth, K. (1995) *Nucleic Acids Symp. Ser. No. 33*, 176–178.
25. Yan, W., and Francklyn, C. (1994) *J. Biol. Chem.* 269, 10022–10027.
26. Arnez, J. G., Augustine, J. G., Moras, D., and Francklyn, C. S. (1997) *Proc. Natl. Acad. Sci. U.S.A.* 94, 7144–7149.
27. Rudinger, J., Florentz, C., and Giege, R. (1994) *Nucleic Acids Res.* 22, 5031–5037.
28. Cusack, S., Yaremchuk, A., and Tukalo, M. (1996) *EMBO J.* 15, 6321–6334.
29. Eiler, S., Dock-Bregeon, A., Moulinier, L., Thierry, J., and Moras, D. (1999) *EMBO J.* 18, 6532–6541.
30. Shiba, K., Stello, T., Motegi, H., Noda, T., Musier-Forsyth, K., and Schimmel, P. (1997) *J. Biol. Chem.* 272, 22809–22816.
31. Sankaranarayanan, R., Dock-Bregeon, A.-C., Romby, P., Caillet, J., Springer, M., Rees, B., Ehresmann, C., Ehresmann, B., and Moras, D. (1999) *Cell* 97, 371–381.
32. Cavarelli, J., Rees, B., Ruff, M., Thierry, J. C., and Moras, D. (1993) *Nature* 362, 181–184.
33. Musier-Forsyth, K., Stehlin, C., Burke, B., and Liu, H. (1997) *Nucleic Acids Symp. Ser. No. 36*, 5–7.
34. Stehlin, C., Burke, B., Yang, F., Liu, H., Shiba, K., and Musier-Forsyth, K. (1998) *Biochemistry* 37, 8605–8613.
35. Steer, B. A., and Schimmel, P. (1999) *Biochemistry* 38, 4963–4971.
36. Wakasugi, K., Quinn, C. L., Tao, N., and Schimmel, P. (1998) *EMBO J.* 17, 297–305.
37. Auld, D. S., and Schimmel, P. (1995) *Science* 267, 1994–1996.
38. Shi, J. P., Musier-Forsyth, K., and Schimmel, P. (1994) *Biochemistry* 33, 5312–5318.
39. Ibba, M., Sever, S., Praetorius-Ibba, M., and Söll, D. (1999) *Nucleic Acids Res.* 27, 3631–3637.
40. Nicholls, A., Sharp, K. A., and Honig, B. (1991) *Proteins: Struct., Funct., Genet.* 11, 281–286.

BI0025316